Geographical Research

Dynamics of Land Surface Temperature in Response to Land-Use/Cover Change

XIAOLU ZHOU[1]* and YI-CHEN WANG[2]
[1]*Department of Geography, National University of Singapore, 1 Arts Link, AS2 #03-01, Singapore, 117570.*
[2]*Department of Geography, National University of Singapore, 1 Arts Link, AS2 #03-05, Singapore, 117570.*
**Corresponding author. Email: g0800627@nus.edu.sg; xiaoluzhou86@gmail.com*

Received 21 July 2010; Revised 10 October 2010; Accepted 14 November 2010

Abstract
In this study, we employed Geographical Information Systems and remote sensing techniques to investigate the impact of land-use/cover change on land surface temperature (LST) in a rapidly urbanisation city, Kunming in southwest China. Spatial patterns of LST and land use for 1992 and 2006 were derived from Landsat images to examine how LST responded to urban growth. Remote sensing indices were used to quantify land-use types and employed as explanatory variables in LST modelling. The geographically weighted regression (GWR), a location dependent model, was performed to explore the influences of the spatially varied land-use conditions on the LST patterns. Results revealed that rapid urbanisation in Kunming altered the local thermal environment, particularly in increasing the LST in the zone surrounding the urban core. Remote sensing indices demonstrated that water and vegetation played an important role in mitigating the urban heat island effect, while built-up and barren land accounted for the increase in LST. The GWR improved the goodness-of-fit for LST modelling and provided insights into the spatially varied relationship between LST and land-use conditions.

KEY WORDS *land-use/cover change; urban heat island; remote sensing; geographical information systems; geographically weighted regression; Kunming*

Introduction

Rapid population growth and continuous exploitation of natural resources during the past century have caused land-use/cover change (LUCC) worldwide. Urbanisation is occurring in many countries, increasing the concentration of population in cities. The rate of urbanisation in some developing countries is remarkable over recent decades because of the pursuit of fast economic development (Li *et al*., 2009). In China, the launch of economic reforms since the late 1970s has largely accelerated the urbanisation process (Luo and Wei, 2009).

The process of urbanisation often replaces natural vegetation and agricultural land with impervious surfaces, such as buildings and roads (Thi Van and Xuan Bao, 2010). This trend has produced a series of environmental impacts on biodiversity, local climate, hydrologic processes, and so forth (Streutker, 2002; Roy *et al*., 2009). Of these impacts, the urban heat island (UHI), the phenomenon where temperatures in urban cores are higher than they are in surrounding rural areas (Voogt and Oke, 2003), is commonly associated with cities. Because each land-use/cover type has its unique thermal, moisture, and

optical spectral properties, LUCC will affect the local thermal environment (Oke, 1982). For example, the expansion of the impervious surface area alters the heat capacity and radiative properties of the land surface, largely reducing the evapotranspiration in urban areas (Streutker, 2002).

Prior studies on urban thermal environments have been based on air temperature obtained from weather stations (Li *et al*., 2009). Although these *in situ* data can provide accurate local temperature, they are normally costly for large-scale analyses and subject to private or governmental restrictions (Owen *et al*., 1998). Furthermore, data from weather stations are discrete points in space, which hardly reflect the spatial variation of temperature caused by different land-use/cover types. An alternative to measuring urban thermal environment is using land surface temperature (LST) because it is able to modulate the air temperature of the layer immediately above the earth surface and is a major parameter associated with surface radiation and energy exchange (Voogt and Oke, 1998; Weng, 2009). A variety of satellite sensors that capture thermal infrared information have been available, such as Landsat Thematic Mapper (TM) and Enhanced Thematic Mapper Plus, and Moderate-resolution Imaging Spectroradiometer, facilitating the investigation of LST in high spatial and temporal resolutions.

Studies have investigated the relationship between LST and LUCC (Chen *et al*., 2006; Xiao and Weng, 2007; Thi Van and Xuan Bao, 2010) with two main foci. The first focus has been on the comparison of the LST of different land-use conditions. Multispectral techniques have been used because thermal and land-use information can be obtained simultaneously from a single sensor (Voogt and Oke, 2003). Analytical functions of Geographical Information Systems (GIS), such as spatial overlay and image differencing, coupled with biophysical parameters of surface temperature and emissivity derived from remotely sensed images, have effectively unveiled the impacts of LUCC on thermal environment change (Chen *et al*., 2006).

The second focus has been on modelling LST based on remote sensing indices. Instead of directly using land-use types that are categorical data, remote sensing indices are employed to quantitatively represent land-use/cover types. For example, the Normalized Difference Vegetation Index (NDVI) has been used to validate the role of green space in mitigating UHI (Yuan and Bauer, 2007). The Normalized Difference Built-up Index (NDBI) (Zha *et al*., 2003) and the Normalized Difference Water Index (NDWI) (Gao, 1996) have been employed to represent urban and water areas quantitatively. Although prior studies have adopted these indices to model LST (Chen *et al*., 2006), only a few of them have compared the modelling results of different years.

When modelling the LST, global regression models, such as ordinary least squares regression (OLS), are commonly developed to estimate LST based on explanatory variables (Weng *et al*., 2004; Chen *et al*., 2006). These global models assume that the relationships between LST and explanatory variables are spatially constant (Bagheri *et al*., 2009). However, the explanatory variables, such as land-use/cover types and their changes, often have various effects on LST across the space. Research is thus needed that employs localised statistical models in analysing the relationship between LST and LUCC.

In this study, the effect of LUCC on LST in a rapidly urbanisation city, Kunming, China, was investigated. LST was derived from satellite images, and the change of the LST pattern in response to urbanisation was explored using GIS and remote sensing techniques. Three remote sensing indices were compared in terms of their effectiveness in LST estimation. Effects of spatial variation of land-use/cover distribution on LST were examined by comparing the OLS, a global model, with the geographically weighted regression (GWR), a location dependent method. Specifically, the study addressed three questions. First, how has urbanisation affected the local thermal environment? Second, how effective are different remote sensing indices in LST estimation? Third, does the location dependent GWR method perform better in LST modelling than the OLS method?

Study area

The study area, Kunming, is located from 102°10′ to 103°40′E and 24°23′ to 26°33′N in the north-central Yunnan province, China (Figure 1). It is situated on a plateau with elevation ranging from 1500 m to 2800 m. The metropolitan area of Kunming is located in the Dianchi basin with an elevation of 1890 m, surrounded by mountains to the north, east, and west. The city is characterised by a subtropical highland climate with warm and humid summers and cold and dry winters. Mean annual precipi-

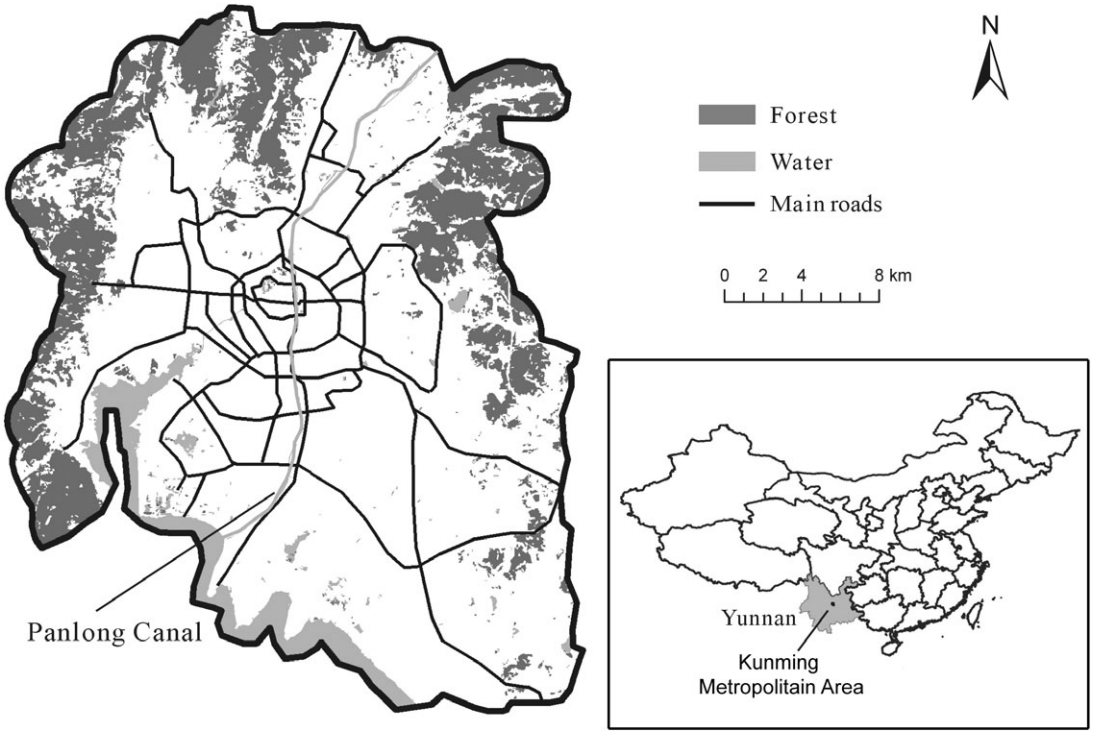

Figure 1 Location of the study area, the Kunming metropolitan area, in Yunnan Province, China.

tation is around 1000 mm; mean annual sun exposure is about 2250 hours.

Kunming is the capital of Yunnan province and has experienced rapid development in the last two decades. The gross domestic product (GDP) increased from 16.9 billion Chinese Yuan in 1992 to 56.2 billion in 1998. From 1998 to 2008, the GDP nearly tripled, attaining 160.5 billion Chinese Yuan (KBS, 2009). The fast economic growth is accompanied by rapid urbanisation, causing a great loss of green space in the suburban areas and an increase of the urbanised area from 184.4 km^2 in 1992 to 257.8 km^2 in 2005 (Cai, 2007). The study area is within metropolitan Kunming, an area of 538.9 km^2, consisting of urban area (dominated by impervious land), urban fringe (combination of impervious land and agriculture land), and suburban area (dominated by forest land).

Materials and methods

Data

Remotely sensed images and field survey data were used in this study. The remotely sensed images used were Landsat 5 TM images obtained from the US Geological Survey website with standard systematic corrections. Because of data quality, availability, and comparability, two scenes of images, dated 16 August 1992 and 19 May 2006, were used in this study. The optical bands of TM images (bands 1–5 and 7) have a spatial resolution of 30 m and the thermal band (band 6) has a spatial resolution of 120 m. Field survey data consisted of ground control points collected using Global Positioning Systems (GPS) for geo-referencing the two TM images and photographs for assisting in image interpretation.

Image preparation

Figure 2 is the flow chart of the analysis. For image preparation, the GPS ground control points were used to geo-reference and rectify the two TM images to the Universal Transverse Mercator coordinate system zone 48, using the WGS84 datum. The nearest neighbour method was employed to resample all the bands into 30 m. The root mean square error was controlled within 0.5 pixels for these two images. To remove the effect of cloud on land-use classification and LST derivation, cloud cover, which

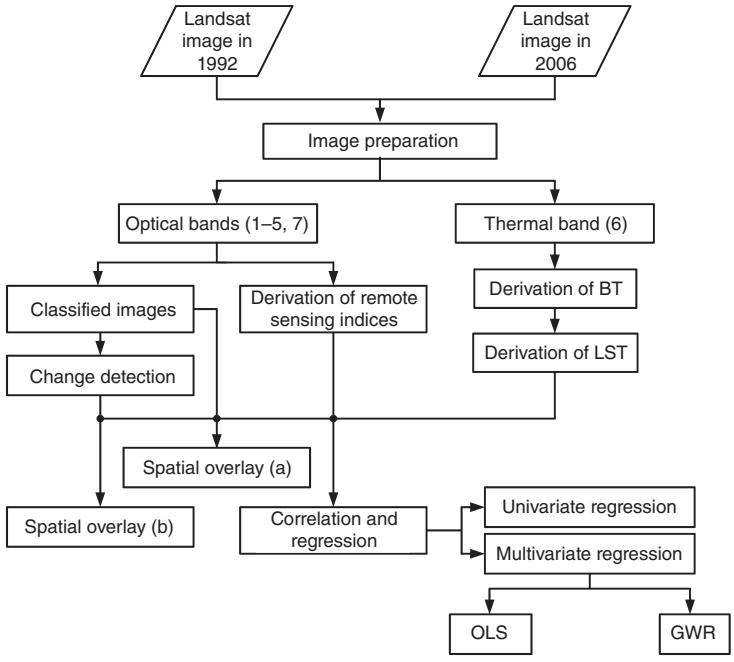

Figure 2 Flow chart of the analysis. Spatial overlay (a) is conducted using the land-use layer and the LST layer, while spatial overlay (b) uses the land-use change layer and the LST layer. BT, brightness temperature; GWR, geographically weighted regression; LST, land surface temperature; OLS, ordinary least squares regression.

accounted for less than 1% of the images, was masked out from the analysis. Atmospheric correction was carried out in ENVI 4.6 using the Fast Line-of-sight Atmospheric Analysis of Spectral Hypercubes (FLAASH) atmospheric correction module to convert digital numbers (DN) into reflectance. FLAASH is an atmospheric correction tool based on the MODTRAN radiation transfer codes and algorithms by which a unique model can be computed for each image (ENVI, 2009). The process filters the interference from the path radiation, such as aerosol, dust particle, and water vapour.

Image classification

The two TM images were classified into five land-use types, including built-up land, water, barren land, forest, and agriculture land, for the assessment of LST change in response to urbanisation. This classification system was feasible considering the medium resolution satellite images used. In addition, it conformed to the Chinese land-use system (SAC, 2007), and a classification system used in prior research whose study area shared the same characteristics as Kunming city (Xiao and Weng, 2007).

The maximum likelihood classifier was employed. Statistics of training samples were plotted to ensure the separability of different classes and comparability between two images (Jensen, 2005). Accuracy assessment was performed using the stratified random sampling method. Field survey assisted by photographs and knowledge of the area were used as references in the assessment. The overall accuracy for the images of 1992 and 2006 was 83.7% and 80.8%, respectively. The Kappa coefficients for both images were above 0.78.

Derivation of LST

The DN values of both Landsat images were converted into spectral radiance based on the following formula:

$$Radiance = gain \times DN + offset \qquad (1)$$

Where, *gain* and *offset* were derived from the head files of images and the Landsat current radiometric calibration coefficients (Chander *et al*., 2009).

The retrieved radiance was converted into at-satellite brightness temperature (BT) based

on the following equation, assuming that land cover had the same emissivity (Weng and Lu, 2008):

$$T_b = \frac{K_2}{\ln(1 + K_1/L_\lambda)} \quad (2)$$

Where T_b is the at-satellite BT in Kelvin (K); L_λ is the spectral radiance in $\mathrm{Wm^{-2}\,sr^{-1}\,\mu m^{-1}}$; K_1 and K_2 are the calibration constants with $K_1 = 607.76\ \mathrm{Wm^{-2}\,sr^{-1}\,\mu m^{-1}}$ and $K_2 = 1260.56$ K.

Because the focus of the study, like most of the prior work (e.g. Weng *et al*., 2004; Chen *et al*., 2006; Li *et al*., 2009), was on the spatial variation of surface temperature, the following methods were employed. To retrieve the LST, the at-satellite BT (T_b) needs to be corrected according to the real object properties. Therefore, the emissivity corrected surface temperature was computed following Artis and Carnahan (1982):

$$T_s = \frac{T_b}{1 + (\lambda \times T_b/\alpha)\ln\varepsilon} \quad (3)$$

Where T_s is the LST in K; λ is the wavelength of emitted radiance ($\lambda = 11.5$ μm) (Markham and Barker, 1985); α equals 1.438×10^{-2} mK, calculated as $\alpha = hc/\sigma$, with h as the Planck constant (6.626×10^{-34} Js), c as the velocity of light (2.998×10^8 m s^{-1}), and σ as the Boltzmann constant (1.38×10^{-23} J/K); ε is the surface emissivity derived from NDVI (Artis and Carnahan, 1982; Roerink *et al*., 2000).

Derivation of remote sensing indices

Three remote sensing indices, NDVI, NDBI, and Modified Normalized Difference Water Index (MNDWI) (Xu, 2006), were computed to characterise the land-use types of this study. The NDVI is an index widely used to describe the greenness of an area (Chen and Brutsaert, 1998), and is used to represent the extent of forest and agricultural land. The NDBI is an indicator of urban areas, which can reveal the built-up and barren land (Zha *et al*., 2003; Chen *et al*., 2006). The MNDWI is selected to represent water areas because water areas often reveal remarkable differences in thermal characteristics when modelling the urban thermal environment, and compared with NDWI, MNDWI can remove the built-up land noise on water in the urban areas (Xu, 2008). These three indices are calculated as follows:

$$NDVI = \frac{R_{NIR} - R_{RED}}{R_{NIR} + R_{RED}} \quad (4)$$

$$NDBI = \frac{R_{MIR} - R_{NIR}}{R_{MIR} + R_{NIR}} \quad (5)$$

$$MNDWI = \frac{R_{GREEN} - R_{MIR}}{R_{GREEN} + R_{MIR}} \quad (6)$$

Where R_{NIR} is the reflectance in the near infrared band; R_{RED} and R_{GREEN}, respectively, stand for the reflectance in red and green bands; R_{MIR} denotes the reflectance in the middle infrared band.

Analysis of the impacts of LUCC on LST

The classified land-use maps and the derived LST layers of 1992 and 2006 were incorporated into ArcGIS 9.3 to analyse the relationship between the spatial patterns of LST and land-use types. Because of spatial autocorrelation, a large portion of the data was redundant for analysis. Spatial sampling was thus carried out to extract 5929 points evenly distributed over the study area for analysis. The LST layers were then imposed onto the land-use layers to explore the average temperature for each land-use type (Spatial overlay (a) in Figure 2). The LSTs of different land-use types in 1992 and 2006 were compared to examine the thermal environment change. To examine how LUCC might have influenced the LST pattern, change detection was performed in ArcGIS to identify the areas where LUCC took place between 1992 and 2006. The detected changed areas were then overlaid with LST layers to calculate the LST differences during this time period (Spatial overlay (b) in Figure 2).

Variation in LST may be subject to three major factors: seasonality, time of day, and land-use condition. To investigate the LST variation associated only with changes in land-use condition, the effects of the other two factors need to be minimised. Since the Landsat satellite follows a sun-synchronous orbit, it ensures that images taken for the same area have a similar local time. The two images used in this study were both captured at around 10:30 AM local time, thereby excluding the influence of the time of day factor. As for seasonality, temperature difference for the same land-use type between the two images in August 1992 and May 2006 was assumed to be caused by different seasons. To exclude the seasonal influence, LST difference for the same

land-use type was normalised against all other LST differences:

$$dT_{ij} = T_{j(2006)} - T_{i(1992)} \quad (7)$$

$$\Delta T_i = T_{i(2006)} - T_{i(1992)} \quad (8)$$

$$dT_n = dT_{ij} - \Delta T_i \quad (9)$$

Where dT_{ij} is the temperature difference between land-use type j in 2006 and land-use type i in 1992; ΔT_i is the temperature difference for the same land-use type i in 2006 and 1992; dT_n is the normalised temperature by subtracting ΔT_i from dT_{ij}.

Univariate and multivariate regression of LST on remote sensing indices

The land-use types of the study area were represented using remote sensing indices of NDVI, NDBI, and MNDWI. Areas with more greenness will exhibit higher NDVI values. High NDBI values generally signify areas with intensive urban development. The MNDWI is sensitive to water bodies, so it will exhibit high values for areas covered by water.

The strength of the correlation between LST and individual explanatory variables (i.e. each of the three remote sensing indices) was first calculated using univariate regression. Multivariate regression was next conducted to model the LST based on the combination of the explanatory variables. The multivariate regressions were performed based on OLS and GWR. As opposed to OLS which may mask out local variation, GWR is a localised regression that examines spatially non-stationary phenomena (Fotheringham *et al*., 2002; Lloyd and Shuttleworth, 2005) and is expressed as:

$$y = \beta_0(u_i, v_i) + \sum_k \beta_k(u_i, v_i) X_{ki} + \varepsilon_i \quad (10)$$

Where β_0 is the constant that depends on the specific location i; β_k is the coefficient of independent variable X_k at the location i; ε_i is the residual term at the location i; (u_i, v_i) indicates the coordinates of the point i. GWR allows local parameters to be estimated based on adjacent points. Coefficient β_k is controlled by the weight which is assigned according to the spatial proximity of point i to its adjacent points. Weight can be obtained through two types of functions, fixed or adaptive (Páez *et al*., 2002a; 2002b). In this study, an adaptive function is used which takes on the form below (Fotheringham *et al*., 2002):

$$w_{ij} = \left[1 - \left(\frac{d_{ij}}{b}\right)^2\right]^2 \quad if \quad j \in \{S\}$$
$$w_{ij} = 0 \quad otherwise \quad (11)$$

Where d_{ij} is the distance from point i to j; S is the set that indicates the specified N nearest neighbour points; b is the bandwidth, defined as the distance from the Nth nearest neighbor point to i. The corrected Akaile Information Criterion (AICc), an indicator of the distance between the unknown 'true' model and the derived model (Fotheringham *et al*., 2002), was used to determine the bandwidth. A lower value of AICc generally reflects a better simulation; thus, following Charlton and Fotheringham (2009), a computational process was done for each point to search for the lowest AICc to determine the corresponding bandwidth.

To evaluate the robustness of the spatial regressions, the spatial distribution of residuals from OLS and GWR were analysed. If the residuals cluster together and display an obvious spatial pattern, the constructed model may be in question. Moran's I, an index that measures the correlation degree of the adjacent observations, was used. The index ranges from −1 (perfect negative autocorrelation) to 1 (perfect positive autocorrelation) with values close to zero suggesting no obvious spatial autocorrelation.

Results

Impacts of LUCC on LST

The LST maps of 1992 and 2006 (Figure 3) not only exhibited the magnitude and spatial variation of surface temperature, but also showed the effects of urbanisation on LST. The central urbanised area with a light tone indicated a warmer surface temperature. The area with light tone spread dramatically from 1992 to 2006, suggesting the expansion of UHI.

The spatial pattern change of the remote sensing indices also revealed the effect of LUCC on LST (Figure 4). Areas with high NDVI shrank tremendously from 1992 to 2006, suggesting a green space loss (Figure 4a). Light tones in the NDBI maps signified the urbanised areas (Figure 4b), and they showed a marked urban growth from 1992 to 2006. These results echoed

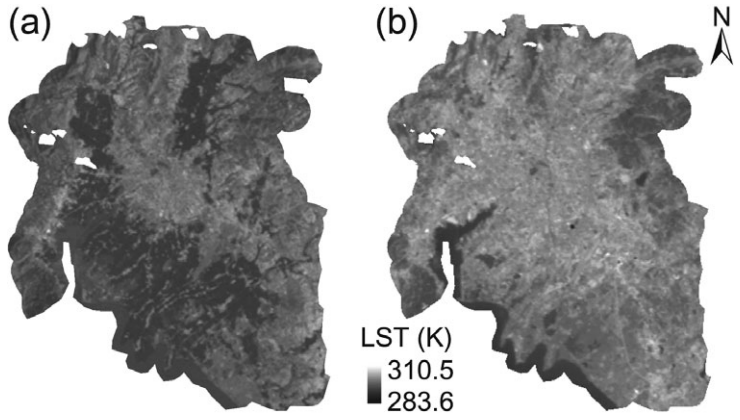

Figure 3 Land surface temperature (LST) in (a) 1992 and (b) 2006. K, Kelvin degrees.

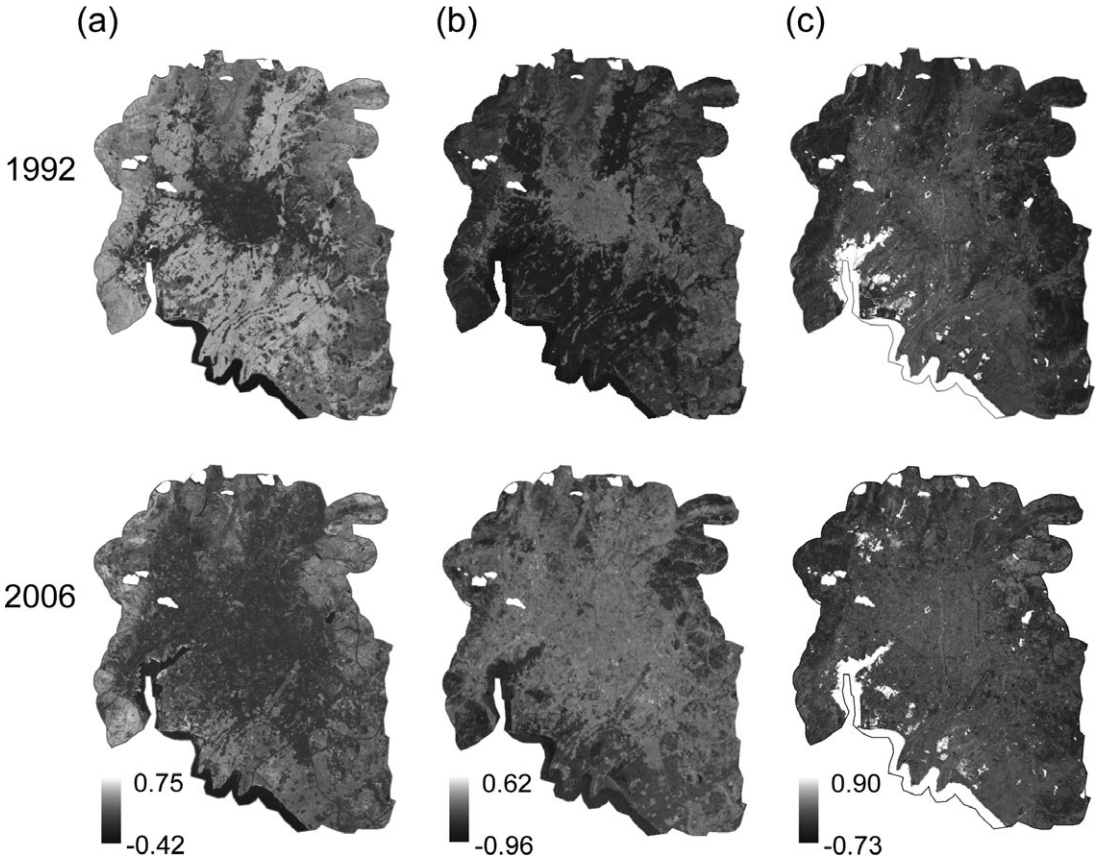

Figure 4 Remote sensing indices of (a) Normalized Difference Vegetation Index; (b) Normalized Difference Built-up Index; and (c) Modified Normalized Difference Water Index in 1992 and 2006.

the increased LST in the urban fringe (Figure 3). The MNDWI maps reflected the water areas, but did not display any major pattern change during the time period (Figure 4c).

The LST maps of the two years were superimposed onto land-use maps to retrieve the surface temperature for each land-use type. Of all the five land-use classes, water exhibited the lowest tem-

perature with the minimum variation between the two years because its relatively high thermal inertia reduced the heat difference. Built-up and barren land showed the highest temperatures in 1992 and 2006. The temperature of forest was between that of water area and built-up land, with a 1.3 K difference between 1992 and 2006, indicating a relatively stable thermal environment for forested land. Agricultural land exhibited a great thermal difference of 5 K between the two years, probably due to the different crop growing stages. In August, crops in Kunming are in their prime time so agricultural land is covered by full green vegetation. While in May, crops are just planted, with much of the land still covered by soil. This resulted in a large temperature difference between the two dates for agricultural land (Table 1).

To investigate the effect of LUCC on LST change, differences in LST were calculated by subtracting LST in 1992 from LST in 2006 for each land-use change category (Table 2). LST increased about 3.4 K and 1.9 K, respectively, for forest and agricultural land that were converted into built-up areas. The LST dropped 3.1 K when agricultural land changed to forest, but rose 1.5 K when forest was turned

Table 1 Derived land surface temperature in Kelvin degrees for each land-use type with the standard deviation in parentheses.

Land-Use Types	16 August 1992	19 May 2006	*dT*
Agriculture	293.8 (1.5)	298.9 (1.7)	5.1
Water	292.4 (1.1)	291.7 (1.0)	–0.7
Barren	297.6 (2.1)	300.4 (2.0)	2.8
Built-up	298.3 (2.2)	301.0 (2.0)	2.7
Forest	295.1 (2.1)	296.4 (2.0)	1.3

dT is the temperature difference between 1992 and 2006.

Table 2 Effects of land-use/cover change on land surface temperature.

Land-Use Type		*dT* (s.d.)	Adjusted *dT*
16 August 1992	19 May 2006		
Agriculture	Agriculture	4.7 (2.2)	0
	Built-up	6.6 (2.7)	1.9
	Barren	7.1 (2.4)	2.4
	Water	–2.8 (1.7)	–7.5
	Forest	1.6 (2.2)	–3.1
Forest	Forest	1.7 (2.2)	0
	Built-up	5.1 (2.8)	3.4
	Barren	4.8 (3.0)	3.1
	Water	–0.7 (1.7)	–2.4
	Agriculture	3.2 (1.8)	1.5
Built-up	Built-up	3.0 (1.9)	0
	Agriculture	2.8 (2.2)	–0.2
	Barren	3.5 (2.7)	0.5
	Water	–1.4 (1.5)	–4.4
	Forest	1.7 (1.0)	–1.3
Barren	Barren	2.0 (2.4)	0
	Built-up	3.7 (2.3)	1.7
	Agriculture	1.7 (2.4)	–0.3
	Water	–1.5 (1.4)	–3.5
	Forest	–0.6 (2.2)	–2.6
Water	Water	–0.9 (0.9)	0
	Barren	3.3 (4.6)	4.2
	Forest	1.2 (1.8)	2.1
	Built-up	4.3 (4.6)	5.2
	Agriculture	4.9 (3.3)	5.8

dT is the temperature difference between two years with standard deviation (s.d.) in parentheses. Adjusted *dT* is calculated based on equations (7)–(9).

into agricultural land. The conversion of barren land had two main pathways. For barren land converted into built-up land, an average of 1.7 K was gained, while for barren land changed into green space, a temperature decline was observed. A small fraction of the built-up land in 1992 changed into green space in 2006, accompanied by a decreased LST.

To highlight the spatial correspondence between LST and LUCC, the land-use types of built-up land and barren land were combined as non-vegetated areas, and forest and agriculture land were combined as vegetated areas. The results exhibited a noticeable correspondence between LUCC and LST change. It was evident that urban sprawl took place on the fringes of the Kunming city from 1992 to 2006, converting vegetated areas into built-up or barren lands, while some non-vegetated areas were turned into vegetated areas in eastern Kunming (Figure 5a). The thermal environment changed accordingly, as seen in the increased LST in the surroundings of the urban core and the decreased LST in eastern Kunming.

Univariate modelling of LST based on remote sensing indices

To better understand how LST dynamics were associated with LUCC, correlation strength between LST and remote sensing indices was examined. Scatter plots of LST and remote sensing indices assessed the effectiveness of each index in modelling LST (Figure 6). For NDVI values above zero, a negative relation with LST was found, suggesting that densely vegetated areas were associated with lower LST. For NDVI values below zero, there were some scattered points deviating from the trend line, probably due to the presence of water that had a lower LST than other land-use types (cf., Table 1). The LST displayed a positive relationship with NDBI. The correlation coefficient increased from 0.55 to 0.59 from 1992 to 2006, suggesting that the NDBI performed better when urban areas became dominant. MNDWI showed a negative relation with LST, which confirmed that water areas had a notably cooling effect. However, the robustness of the regression was reduced by the large variation of LST where MNDWI was below zero.

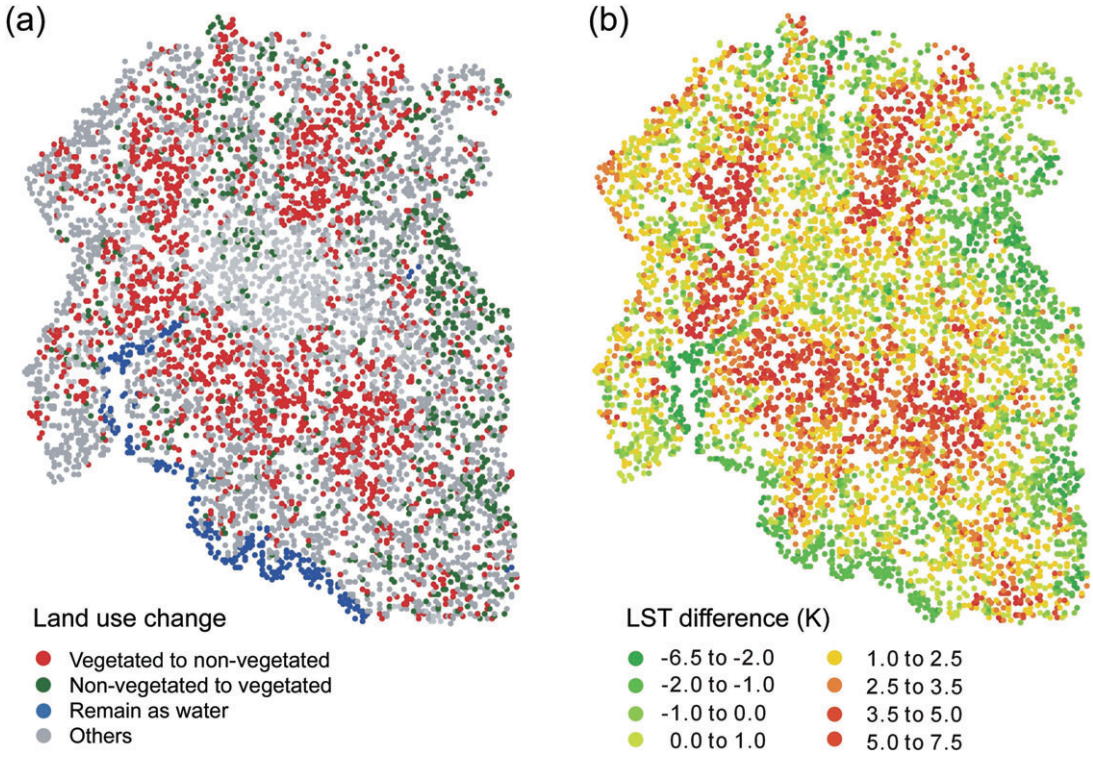

Figure 5 Spatial correspondence between (a) changes in land use and (b) differences in land surface temperature (LST) between 1992 and 2006. Each dot represents one of the 5929 sampled points. K, Kelvin degrees.

Comparison of the OLS and the GWR modelling on LST

Multivariate regression was carried out to examine whether it would improve the LST modelling. When the multivariate regression operated based on the OLS method, results did not reveal a significant improvement. The MNDWI was not statistically significant at the 0.05 level in 1992 (Table 3). Because of the heterogeneity of the land-use mosaic and the spatial variation in LST, the spatially varied relationship between LST and remote sensing indices cannot be reflected by the global modelling method. Conversely, the results of the localised regression method GWR showed a much higher adjusted r^2 value than the OLS (Table 4). The performance of OLS and GWR were further compared using the AICc indicator; the AICc values for GWR were much lower than those for OLS, suggesting that GWR performed better than OLS (Table 4). Results from Moran's I did not show any spatial autocorrelation among the residuals of the OLS and GWR models, indicating the robustness of the models (Table 4).

While the global regression of OLS uniformly showed that high NDVI values were associated with low LST (Table 3), GWR

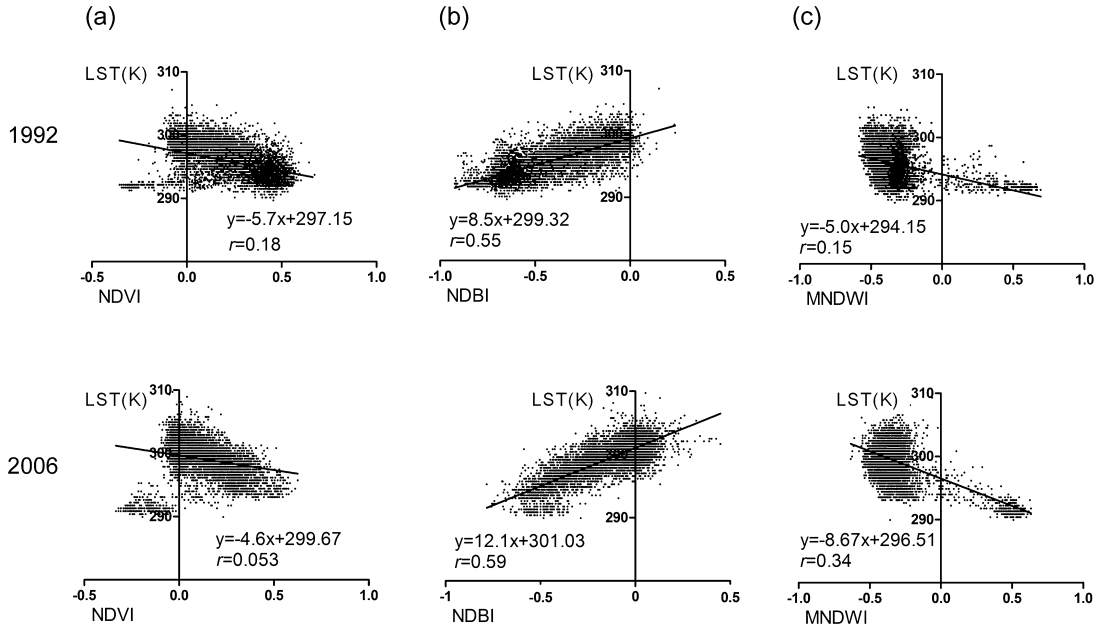

Figure 6 Relations between (a) NDVI and LST; (b) NDBI and LST; and (c) MNDWI and LST. K, Kelvin degrees; LST, land surface temperature; MNDWI, Modified Normalized Difference Water Index; NDBI, Normalized Difference Built-up Index; NDVI, Normalized Difference Vegetation Index.

Table 3 Parameter coefficients of the multivariate regression models based on the OLS and GWR methods.

Coefficients	1992		2006	
	OLS	GWR (Median)	OLS	GWR (Median)
Intercept	299.131	298.512	298.907	299.767
NDVI	0.141	−5.150	−2.827	−4.036
NDBI	8.431	7.984	7.557	7.603
MNDWI	−0.422[1]	−6.083	−5.778	−4.315

[1] Parameter is not significant based on the t statistic (at the 0.05 level).

GWR, geographically weighted regression; MNDWI, Modified Normalized Difference Water Index; NDBI, Normalized Difference Built-up Index; NDVI, Normalized Difference Vegetation Index; OLS, ordinary least squares regression.

allowed the spatially varied relationship between NDVI and LST to be revealed. In most places, coefficients of NDVI displayed as negative values, suggesting that vegetated areas (often high NDVI) relieved the urban heat (thus low LST) (Figure 7a). However, the coefficients of GWR revealed that there were areas with positive coefficients between NDVI and LST, particularly in areas covered by water (cf., Figures 1 and 7a). This illustrated that GWR effectively modelled the relationship between LST and NDVI in areas with different land surface characteristics.

Table 4 Comparison of the diagnostics for OLS and GWR modelling.

Year	Method	Adjust r^2	AICc	Moran's I
1992	OLS	0.531	28 128.7	–0.018
	GWR	0.721	23 046.1	–0.003
2006	OLS	0.615	28 322.6	–0.009
	GWR	0.746	22 668.1	–0.004

AICc, corrected Akaile Information Criterion; GWR, geographically weighted regression; OLS, ordinary least squares regression.

Coefficients of NDBI showed a positive relationship with LST across the study area (Figure 7b). The coefficients increased from 1992 to 2006 in southern Kunming where large areas of agricultural land was converted into urban areas, indicating the effect of urban expansion on enhancing the LST. Apart from representing water area, MNDWI can be used to represent surface moisture (Zha *et al*., 2003; Chen *et al*., 2006). The general negative coefficient of MNDWI (Figure 7c) thus suggested that water bodies and surface moisture can moderate the surface temperature. The comparison of the MNDWI coefficients between 1992 and 2006 showed that areas with positive coefficients of MNDWI expanded in the south-east, inferring a loss of surface moisture because of the

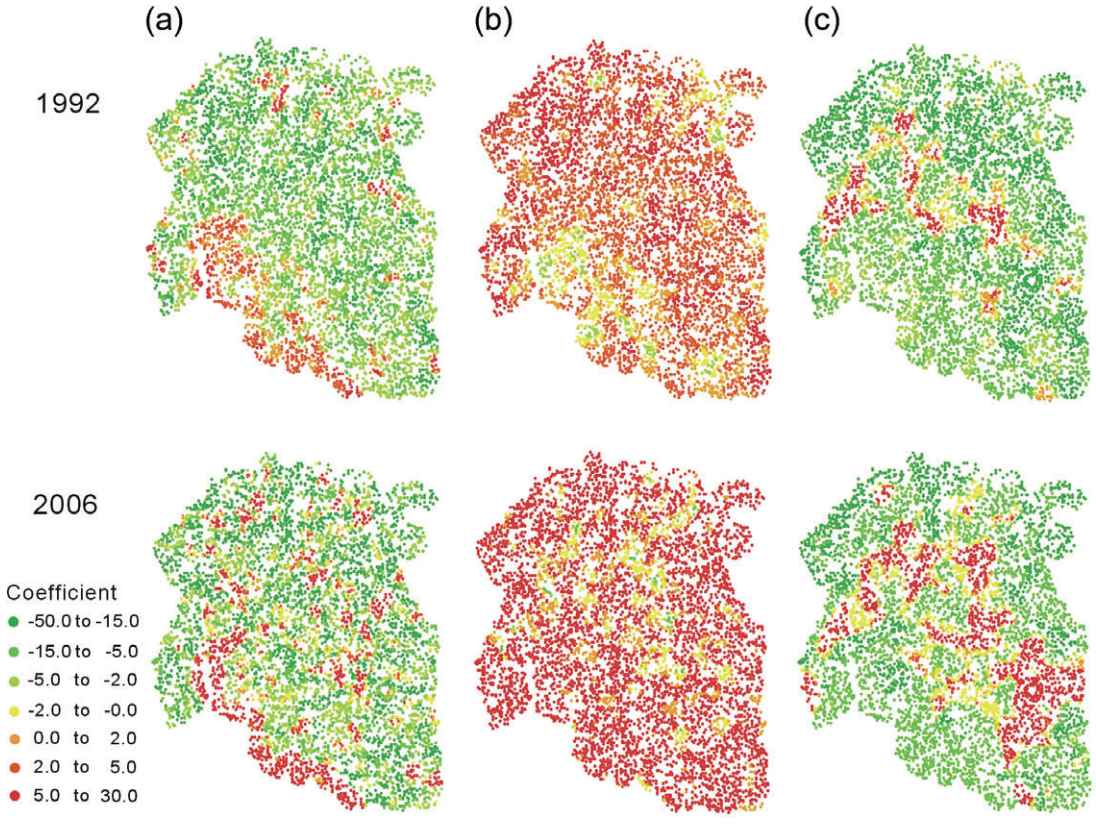

Figure 7 Local coefficients of the geographically weighted regression for (a) Normalized Difference Vegetation Index; (b) Normalized Difference Built-up Index; and (c) Modified Normalized Difference Water Index.

conversion of vegetated land to impervious surface (Figure 7c).

Discussion

Process of thermal environment change

The LUCC has extensively modified the thermal environment of the Kunming city. The LST became higher as the land use changed from vegetated areas to barren and built-up land (Table 2, Figure 5) in the following process. At the beginning stage, the removal of vegetated areas changed the surface energy balance, which increased the sensible heat flux at the cost of the latent heat flux (Owen *et al*., 1998). The evapotranspiration of vegetation was substantially reduced. Following this stage was a conversion of bare soil into impervious surface, which altered the moisture balance. The reduction of the water storage of land further strengthened the sensible heat flux. In addition, the land surface conversion largely modified the thermal property of the land surface (e.g. heat capacity and thermal conductivity), creating a warmer thermal environment (Li *et al*., 2009). At the last stage, a great deal of impervious surface was developed. Built-up areas might facilitate sunlight absorption because of multiple times of reflections. This urban topography, known as the 'canyon effect', further intensified the UHI (Oke, 1982). Apart from land-use change, urbanisation with increased human population also contributed to the urban thermal environment change with the rising anthropogenic heat discharge.

Effects of green policies on the thermal environment

Although areas with high LST have increased from 1992 to 2006 (Figure 3), several spots with dark tone indicating a low LST can be detected in the urban area in 2006 (Figure 3b). These areas were associated with urban parks and riparian belts with vegetation cover. In recent years, Kunming implemented several policies to introduce green space into the city. The campaigns to allot more green patches and corridors into the city ameliorated the urban environment because of the role of vegetation in mitigating UHI, as seen that the temperature of vegetated areas was around 3–4 K lower than the built-up land (Tables 1 and 2). As a result, more cooling spots in the urban core appeared on the 2006 LST map (Figure 3b). The dark line going through the urban centre in Figure 3b showing the position of the Panlong Canal also became noticeable in 2006, suggesting a cooling trend along the Panlong Canal (Figures 1 and 3). This was probably because of the greening initiatives along the banks of the Panlong Canal, which expanded the green strips and thereafter reduced the LST. Also, the greening initiatives implemented in the east of Kunming created or enlarged several urban parks. Accordingly, some barren lands were converted into vegetated areas and noticeably reduced the surface temperature in eastern Kunming (Figure 5).

Localised statistics in LST modelling

Prior studies pointed out that a single remote sensing index could not reflect the combined impacts of vegetation, buildings, water bodies, and other land cover on LST (Buyantuyev and Wu, 2010). Multivariate regression conducted in this study confirmed the importance of combining remote sensing indices in LST modelling. The global models based on the OLS method failed to capture the spatial variation of LST because all the parameters were uniformly applied to the data points regardless of their locations. In contrast, GWR provided local coefficients and residuals, allowing comparison of the modelling results in different places. The local coefficients could be visualised on maps to illustrate the spatially varied relationship between each of the remote sensing indices and LST (Figure 7). The increased values of AICc and the adjusted r^2 both suggested the effectiveness of GWR in LST modelling.

Conclusion and future work

This study contributed to the understanding of LUCC on the thermal environment. Rapid urbanisation notably caused the increase of LST in Kunming, China, particularly in the area surrounding the urban core. Among the three remote sensing indices examined in the study, NDBI revealed a strong relation with LST. Multivariate regression results showed that the local regression model based on GWR significantly improved the goodness-of-fit and provided insights into the spatially varied relationship between LST and land-use conditions. The findings also suggested that sustainable urban green policies would be important in moderating the urban thermal environment. Because different seasons of remote sensing images may have caused the LST difference in

agricultural land in this study, future research can be conducted to examine how LST varies with different land-use/cover types in different seasons, particularly in the seasonal change of the UHI intensity and the effect of green space in mitigating the UHI.

ACKNOWLEDGMENT

The authors wish to thank the National University of Singapore for providing funding support through the Graduate Research Support Scheme and the research grant R-109-000-070-101 and two anonymous reviewers for their insightful comments.

REFERENCES

Artis, D.A. and Carnahan, W.H., 1982: Survey of emissivity variability in thermography of urban areas. *Remote Sensing of Environment* 12, 313–329.

Bagheri, N., Holt, A. and Benwell, G.L., 2009: Using geographically weighted regression to validate approaches for modelling accessibility to primary health care. *Applied Spatial Analysis* 2, 177–194.

Buyantuyev, A. and Wu, J., 2010: Urban heat islands and landscape heterogeneity: linking spatiotemporal variations in surface temperatures to land-cover and socioeconomic patterns. *Landscape Ecology* 25, 17–33.

Cai, H., 2007: Land use change comparative study of Kunming City based on remote sensing. *Guizhou Science* 25, 178–184. (In Chinese).

Chander, G., Markham, B.L. and Helder, D.L., 2009: Summary of current radiometric calibration coefficients for Landsat MSS, TM, ETM+, and EO-1 ALI sensors. *Remote Sensing of Environment* 113, 893–903.

Charlton, M. and Fotheringham, A.S., 2009: Geographically weighted regression white paper. National Centre for Geocomputation, National University of Ireland Maynooth Maynooth, Co Kildare, Ireland, 1–17.

Chen, D. and Brutsaert, W., 1998: Satellite-sensed distribution and spatial patterns of vegetation parameters over a tallgrass prairie. *Journal of the Atmospheric Sciences* 55, 1225–1238.

Chen, X., Zhao, H., Li, P. and Yin, Z., 2006: Remote sensing image-based analysis of the relationship between urban heat island and land use/cover changes. *Remote Sensing of Environment* 104, 133–146.

ENVI, 2009: Atmospheric Correction Module: QUAC and FLAASH User's Guide.

Fotheringham, A.S., Brunsdon, C. and Charlton, M.E., 2002: *Geographically Weighted Regression: The Analysis of Spatially Varying Relationships*. Wiley, Chichester.

Gao, B.-C., 1996: NDWI – A normalized difference water index for remote sensing of vegetation liquid water from space. *Remote Sensing of Environment* 58, 257–266.

Jensen, J.R., 2005: *Introductory Digital Image Processing A Remote Sensing Perspective*, 3th edn. Prentice Hall, Upper Saddle River, NJ.

KBS (Kunming Bureau of Statistics), 2009: *Kunming Statistical Year Book*. China Statistics Press, Beijing. (In Chinese).

Li, J.-J., Wang, X.-R., Wang, X.-J., Ma, W.-C. and Zhang, H., 2009: Remote sensing evaluation of urban heat island and its spatial pattern of the Shanghai metropolitan area, China. *Ecological Complexity* 6, 413–420.

Lloyd, C. and Shuttleworth, I., 2005: Analysing commuting using local regression techniques: Scale, sensitivity, and geographical patterning. *Environment and Planning A* 37, 81–103.

Luo, J. and Wei, Y.H.D., 2009: Modeling spatial variations of urban growth patterns in Chinese cities: The case of Nanjing. *Landscape and Urban Planning* 91, 51–64.

Markham, B.L. and Barker, J.K., 1985: Spectral characteristics of the LANDSAT Thematic Mapper Sensors. *International Journal of Remote Sensing* 6, 697–716.

Oke, T.R., 1982: The energetic basis of the urban heat island. *Quarterly Journal of the Royal Meteorological Society* 108, 1–24.

Owen, T.W., Carlson, T.N. and Gillies, R.R., 1998: An assessment of satellite remotely-sensed land cover parameters in quantitatively describing the climatic effect of urbanization. *International Journal of Remote Sensing* 19, 1663–1681.

Páez, A., Uchida, T. and Miyamoto, K., 2002a: A general framework for estimation and inference of geographically weighted regression models 1, Location-specific kernel bandwidths and a test for locational heterogeneity. *Environment and Planning A* 34, 733–754.

Páez, A., Uchida, T. and Miyamoto, K., 2002b: A general framework for estimation and inference of geographically weighted regression models. 2. Spatial association and model specification tests. *Environment and Planning A* 34, 883–904.

Roerink, G.J., Su, Z. and Meneti, M., 2000: S-SEBI: A simple remote sensing Algorithm to estimate the surface energy balance. *Physics and Chemistry of the Earth* 25, 147–157.

Roy, A.H., Dybas, A.L., Fritz, K.M. and Lubbers, H.R., 2009: Urbanization affects the extent and hydrologic permanence of headwater streams in a midwestern US metropolitan area. *Journal of the North American Benthological Society* 28, 911–928.

SAC (Standardization administration of the people's republic of China), 2007: *Chinese Current Land Use Classification, GB/T 21010_2007*. Chinese Standard Press, Beijing. (In Chinese).

Streutker, D.R., 2002: A remote sensing study of the urban heat island of Houston, Texas. *International Journal of Remote Sensing* 23, 2595–2608.

Thi Van, T. and Xuan Bao, H.D., 2010: Study of the impact of urban development on surface temperature using remote sensing in Ho Chi Minh City, northern Vietnam. *Geographical Research* 48, 86–96.

Voogt, J.A. and Oke, T.R., 1998: Effects of urban surface geometry on remotely sensed surface temperature. *International Journal of Remote Sensing* 19, 895–920.

Voogt, J.A. and Oke, T.R., 2003: Thermal remote sensing of urban areas. *Remote Sensing of Environment* 86, 370–384.

Weng, Q., 2009: Thermal infrared remote sensing for urban climate and environmental studies: Methods, applications, and trends. *ISPRS Journal of Photogrammetry and Remote Sensing* 64, 335–344.

Weng, Q. and Lu, D., 2008: A sub-pixel analysis of urbanization effect on land surface temperature and its interplay with impervious surface and vegetation coverage in Indianapolis, United States. *International Journal of Applied Earth Observation and Geoinformation* 10, 68–83.

Weng, Q., Lu, D. and Schubring, J., 2004: Estimation of land surface temperature–vegetation abundance relationship for urban heat island studies. *Remote Sensing of Environment* 89, 467–483.

Xiao, H. and Weng, Q., 2007: The impact of land use and land cover changes on land surface temperature in a karst

area of China. *Journal of Environmental Management* 85, 245–257.

Xu, H., 2006: Modification of normalized difference water index (NDWI) to enhance open water features in remotely sensed imagery. *International Journal of Remote Sensing* 27, 3025–3033.

Xu, H., 2008: A new index for delineating built-up land features in satellite imagery. *International Journal of Remote Sensing* 29, 4269–4276.

Yuan, F. and Bauer, M.E., 2007: Comparison of impervious surface area and normalized difference vegetation index as indicators of surface urban heat island effects in Landsat imagery. *Remote Sensing of Environment* 106, 375–386.

Zha, Y., Gao, J. and Ni, S., 2003: Use of normalized difference built-up index in automatically mapping urban areas from TM imagery. *International Journal of Remote Sensing* 24, 583–594.